

# Elimination of total internal reflection in GaInN light-emitting diodes by graded-refractive-index micropillars

Jong Kyu Kim,<sup>1,a)</sup> Ahmed N. Noemaun,<sup>1</sup> Frank W. Mont,<sup>1</sup> David Meyaard,<sup>1</sup> E. Fred Schubert,<sup>1</sup> David J. Poxson,<sup>2</sup> Hyunsoo Kim,<sup>3</sup> Cheolsoo Sone,<sup>3</sup> and Yongjo Park<sup>3</sup>

<sup>1</sup>Department of Electrical, Computer, and Systems Engineering, Rensselaer Polytechnic Institute, Troy, New York 12180, USA

<sup>2</sup>Department of Physics, Applied Physics, and Astronomy, Rensselaer Polytechnic Institute, Troy, New York 12180, USA

<sup>3</sup>Central R&D Institute, Samsung Electro-Mechanics, Suwon 443-743, South Korea

(Received 4 November 2008; accepted 13 November 2008; published online 4 December 2008)

A method for enhancing the light-extraction efficiency of GaInN light-emitting diodes (LEDs) by complete elimination of total internal reflection is reported. Analytical calculations show that GaInN LEDs with multilayer graded-refractive-index pillars, in which the thickness and refractive index of each layer are optimized, have no total internal reflection. This results in a remarkable improvement in light-extraction efficiency. GaInN LEDs with five-layer graded-refractive-index pillars, fabricated by cosputtering TiO<sub>2</sub> and SiO<sub>2</sub>, show a light-output power enhanced by 73% and a strong side emission, consistent with analytical calculations and ray-tracing simulations. © 2008 American Institute of Physics. [DOI: 10.1063/1.3041644]

One of the fundamental problems facing light-emitting diodes (LEDs) is the occurrence of trapped light inside the LED, confined by total internal reflection (TIR).<sup>1</sup> Light incident on a planar semiconductor-air or semiconductor-encapsulant interface is totally internally reflected if the angle of incidence is larger than a particular angle called critical angle  $\theta_c$ , resulting in a significant reduction in light-extraction efficiency. In order to extract more light from LEDs, efforts have been ongoing for several decades that included wet-chemical texturing of a LED surface,<sup>2-6</sup> employing periodic photonic crystals,<sup>7,8</sup> planar graded-refractive-index (GRIN) antireflection coatings,<sup>9</sup> patterning of sapphire substrates,<sup>10</sup> and shaping of LED chips.<sup>11</sup>

Wet-chemical texturing of an N-face GaN (000 $\bar{1}$ ) surface of vertical-structured LEDs is known to be very efficient in enhancing light extraction and, hence, is widely used in high-power commercial LEDs.<sup>4,5</sup> However, KOH-based wet-chemical etching needs additional process steps such as deposition and removal of a protection layer covering the Ohmic contact to *n*-type GaN. In addition, due to crystal-plane-dependent etching rates,<sup>3</sup> it is very difficult to form nonrandom, optimized, or designed features. The application of photonic crystals to LEDs has been studied extensively to improve the light-extraction efficiency. However, fabrication of submicron patterns by lithography and plasma dry etching is costly, and the etching process could damage the surface of GaN.

In this work, an effective light outcoupling method for LEDs employing micropatterned GRIN pillars is presented. Analytical calculations and ray-tracing simulations show that with optimized GRIN pillars on GaInN LEDs, no-TIR can be achieved along with a 145% increase in light-extraction efficiency. The experimental increase in light-output power of GaInN LEDs with GRIN pillars is as high as 73%, mediated by enhanced light extraction through the side walls of the GRIN pillars as well as reduced Fresnel reflection for light

transmitted through the top surface of the GRIN pillars.

Let us consider an optical ray entering into a pillar with refractive index  $n_1$  and impinging on the pillar's top surface, as shown in Fig. 1(a). If the ray does not fall within the escape cone, defined by the critical angle  $\theta_c = \arcsin(n_{\text{air}}/n_1)$ , it is reflected back into the semiconductor by TIR. If an

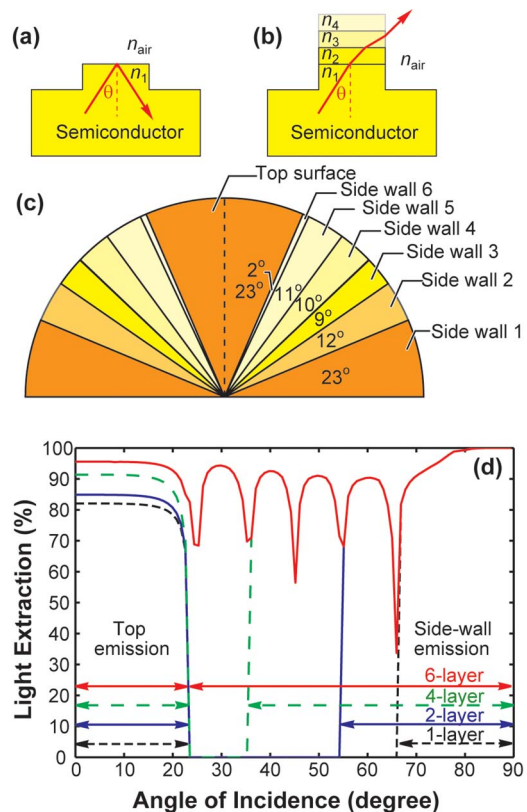


FIG. 1. (Color online) Schematic of (a) one-layer and (b) multilayer GRIN pillars on a semiconductor. (c) Schematic of the surfaces, both top and side wall, of the six-layer GRIN pillar through which each light ray incident at various angles into the pillar gets extracted. (d) Calculated light-extraction efficiency of pillars with various numbers of GRIN layers.

<sup>a)</sup>Electronic mail: kimj4@rpi.edu.

additional layer-2 with refractive index  $n_2$ , slightly lower than  $n_1$ , is formed on the pillar, the ray is refracted, rather than reflected, enters layer-2, and may fall within the escape cone of the side wall and thus may be extracted into air. By adding consecutive layers in which the refractive index of each layer is step graded such that  $n_1 > n_2 > n_3 \cdots > n_{\text{air}}$ , as shown in Fig. 1(b), so that the critical angle between consecutive layers is complementary to the critical angle of the side wall, TIR can be completely avoided.

In order to realize an array of multilayer GRIN pillars with no-TIR and to maximize light-extraction efficiency, several geometric conditions need to be considered: (i) the thickness of each layer should have a minimum value to prevent a light ray from bouncing off the top surface back into the semiconductor without reaching the side wall; (ii) the refractive index of each layer needs to be chosen such that TIR does not occur at the top surface and the side wall; (iii) the light extracted through a pillar could re-enter another neighboring pillar if the height of each pillar is large compared to the spacing between them; (iv) since the light incident on the top surface of the semiconductor between two pillars could get reflected back by TIR, the area of this surface should be minimized. Considering these requirements, an optimum layer sequence of GRIN pillars is determined for a pillar diameter of  $1 \mu\text{m}$  on a semiconductor with a refractive index of 2.47 surrounded by air. We find that a six-layer GRIN pillar with optimized layer thicknesses and refractive indices completely avoids TIR. Figure 1(c) shows the top and side-wall surfaces of the six-layer GRIN pillar, through which light rays incident at any angle on the pillar get extracted. For example, a light ray entering into the pillar with incident angle of  $40^\circ$  will be extracted through the side wall of layer-4. Figure 1(d) shows light-extraction efficiency of GRIN pillars with various numbers of layers, from one layer to six layers, as a function of angle of incidence. As the number of GRIN layers increases, light rays with a wider range of incident angles can be extracted through the side wall of the pillar, and eventually a light ray entering into the pillar with *any* angle of incidence gets extracted with the six-layer design. In addition, light extraction through the top surface as well as the side wall of the pillar increases with increasing number of GRIN layers due to reduced Fresnel reflection,<sup>9</sup> resulting in a remarkable improvement in total light-extraction efficiency.

Monte Carlo ray-tracing simulations are performed using the LIGHTTOOLS modeling software. Three LEDs are simulated: (i) a reference LED without pillars, (ii) a LED with one-layer pillars with the same refractive index as that of GaN, and (iii) a LED with optimized five-layer GRIN pillars. In the simulation, pillars with  $2 \mu\text{m}$  diameter and  $1 \mu\text{m}$  total height are separated by  $2 \mu\text{m}$  spacing over an  $n$ -type GaN side of a thin-film GaInN LED emitting at  $460 \text{ nm}$  ( $1 \times 1 \text{ mm}^2$ ,  $3 \mu\text{m}$  thick) with a planar Ag reflector on  $p$ -type GaN. Figure 2 shows the simulated far-field emission intensity of the three LEDs. The LED with five-layer GRIN pillars shows a 145% increase in light extraction compared to a 40% increase shown by single-layer pillars in comparison with the reference LED. Note that the emission through the pillar side wall is much more enhanced than the top emission, consistent with the theoretical calculations shown in Fig. 1.

In order to experimentally demonstrate the viability of the GRIN pillars, thin-film GaInN LEDs emitting at  $460 \text{ nm}$

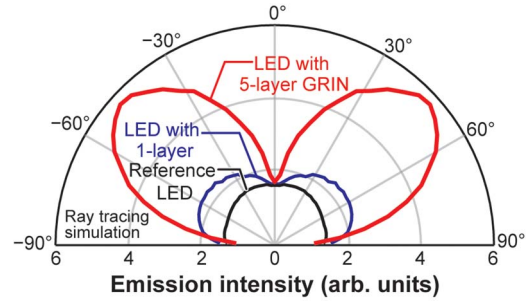


FIG. 2. (Color online) Calculated far-field emission intensities from LEDs using ray-tracing simulation.

were fabricated. The GaInN LED structure was grown by metal-organic vapor phase epitaxy on a  $c$ -plane sapphire substrate and consists of a  $3\text{-}\mu\text{m}$ -thick  $n$ -type GaN buffer layer, an  $n$ -type GaN lower cladding layer, a GaInN/GaN multiple quantum-well active region, a  $p$ -type AlGaIn electron blocking layer, and a  $p$ -type GaN upper cladding layer. For electrical isolation, a square-shaped mesa structure is obtained by inductively coupled plasma etching down to the sapphire substrate, followed by deposition of a  $400\text{-nm}$ -thick  $\text{SiO}_2$  passivation film by plasma-enhanced chemical vapor deposition. Prior to the metal deposition on  $p$ -type GaN, the samples were dipped in HCl solution for 1 min to remove surface oxide layers. A  $300\text{-nm}$ -thick Ag-based reflective Ohmic contact was deposited on  $p$ -type GaN by an electron-beam evaporation system, followed by rapid-thermal annealing at  $550^\circ\text{C}$  for 1 min under air to form a low resistance, highly reflective Ohmic contact to  $p$ -type GaN.<sup>12,13</sup> Then, a Ni/Au conductive seed layer was deposited on an entire wafer, followed by the electroplating a  $40\text{-}\mu\text{m}$ -thick Ni layer. A KrF excimer laser was used for a laser lift-off process to separate the GaN from the sapphire substrate. The separated nitrogen-face GaN was etched to expose the  $n$ -type GaN layer, on which a Cr/Au Ohmic contact was deposited. Arrays of pillar patterns with various sizes ( $2 \times 2$ ,  $5 \times 5$ , and  $10 \times 10 \mu\text{m}^2$ ) and spacings between pillars ( $2$  and  $5 \mu\text{m}$ ) were formed on an array of  $1 \times 1 \text{ mm}^2$  LEDs along with reference LEDs by standard photolithography. Then a five-layer GRIN film was deposited by cosputtering  $\text{TiO}_2$  and  $\text{SiO}_2$  sputtering targets, in which the refractive indices of the composite materials,  $(\text{TiO}_2)_x(\text{SiO}_2)_{1-x}$ , are precisely tuned to desired values by adjusting the electrical power for two sputtering targets.<sup>14</sup> As shown in Table I, both the thickness and the refractive index of each layer are well controlled to values close to calculated target values. Figure 3 shows a scanning electron micrograph of the LED with five-layer GRIN

TABLE I. Designed and measured thicknesses and refractive indices of five-layer graded-refractive-index pillars deposited by cosputtering of  $\text{TiO}_2$  and  $\text{SiO}_2$ .

Layer	Materials deposited by cosputtering	Designed		Measured	
		Thickness (nm)	Refractive index	Thickness (nm)	Refractive index
1	$\text{TiO}_2$	331	2.47	415	$\sim 2.47$
2	$(\text{TiO}_2)_x(\text{SiO}_2)_{1-x}$	317	2.26	282	2.34
3	$(\text{TiO}_2)_x(\text{SiO}_2)_{1-x}$	297	2.02	282	2.02
4	$(\text{TiO}_2)_x(\text{SiO}_2)_{1-x}$	269	1.76	267	1.75
5	$\text{SiO}_2$	219	1.45	238	$\sim 1.45$

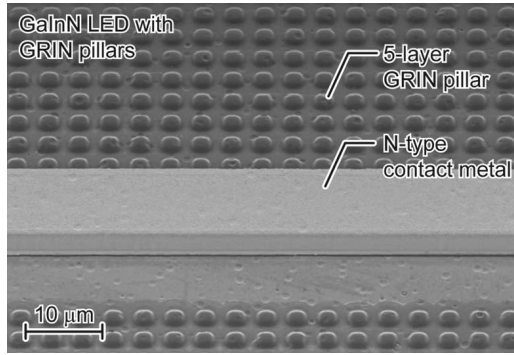


FIG. 3. Scanning electron micrograph of the LEDs with five-layer GRIN pillars with  $2 \times 2 \mu\text{m}^2$  area and  $2 \mu\text{m}$  spacing.

pillars with a  $2 \times 2 \mu\text{m}^2$  size and  $2 \mu\text{m}$  spacing.

The angular-dependent electroluminescence intensity of 63 representative LED chips with different pillar sizes and spacings was measured using a blue-enhanced Si *p-i-n* photodetector. The relative light-output power of the GaInN LEDs with GRIN pillars is significantly higher than that of the reference LEDs, as shown in Fig. 4(a). At an injection current of 20 mA, the enhancement in the light output of the LEDs with  $5 \times 5 \mu\text{m}^2$  area and  $2 \mu\text{m}$  spacing GRIN pillars shows the highest improvement of 73%. Based on our simu-

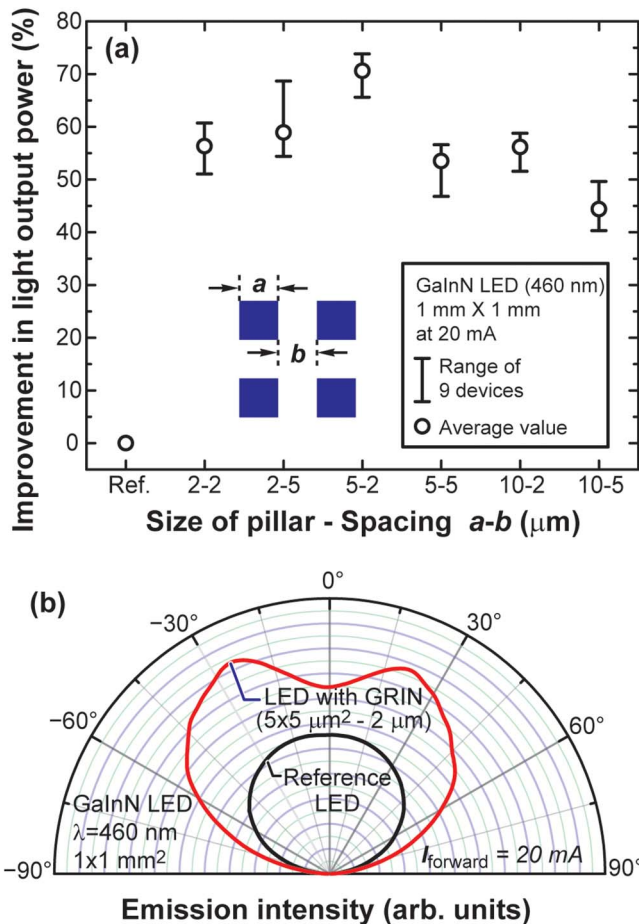


FIG. 4. (Color online) (a) The improvement in light-output power of the GaInN LEDs with GRIN pillars in comparison with that of the reference LEDs. (b) Measured far-field emission intensity from LEDs.

lation, LEDs with  $2 \times 2 \mu\text{m}^2$  area and  $2 \mu\text{m}$  spacing GRIN pillars were expected to show the best result; however, the improvement is less than expected. This is possibly attributed to a reduction in the actual height of  $2 \times 2 \mu\text{m}^2$  pillars due to less materials being deposited through relatively narrow photoresist openings during the cosputtering. Figure 4(b) shows the far-field emission intensity of a reference LED and a LED with GRIN pillars. The emission through the side wall of GRIN pillars is much more enhanced, consistent with analytical calculations and ray-tracing simulations shown in Figs. 1 and 2, respectively. It is anticipated that the light output of the GaInN LEDs with GRIN pillars can be further increased by optimizing the shape and size of the pillars and the spacing between them.

In summary, a promising method for enhancing the light-extraction efficiency of GaInN LEDs by completely eliminating TIR was introduced and demonstrated. Analytical calculations and ray-tracing simulations show that multilayer GRIN pillars, in which the thickness and refractive index of each layer are optimized, on top of a GaN-based LED result in a remarkable improvement in light extraction through the pillar side walls as well as the top surface. Five-layer GRIN pillars were fabricated by cosputtering  $\text{TiO}_2$  and  $\text{SiO}_2$  on top of GaInN LEDs emitting at 460 nm. It is experimentally shown that the enhancement in the light output of the GaInN LEDs with  $5 \times 5 \mu\text{m}^2$  area and  $2 \mu\text{m}$  spacing GRIN pillars is as high as 73%. The strong side emission is consistent with our expectations made by theoretical calculations and ray-tracing simulations.

The authors gratefully acknowledge support from Samsung Electro-Mechanics Company, National Science Foundation (NSF), Sandia National Laboratories, New York State, Crystal IS Corporation, Troy Research Corporation, and the U.S. Department of Energy.

<sup>1</sup>E. F. Schubert, *Light Emitting Diodes*, 2nd ed. (Cambridge University Press, Cambridge, England, 2006).

<sup>2</sup>T. Fujii, Y. Gao, R. Sharma, E. L. Hu, S. P. DenBaars, and S. Nakamura, *Appl. Phys. Lett.* **84**, 855 (2004).

<sup>3</sup>Y. Gao, T. Fujii, R. Sharma, K. Fujito, S. P. Denbaars, S. Nakamura, and E. L. Hu, *Jpn. J. Appl. Phys., Part 2* **43**, L637 (2004).

<sup>4</sup>O. B. Shchekin, J. E. Epler, T. A. Trotter, T. Margalith, D. A. Steigerwald, M. O. Holcomb, P. S. Martin, and M. R. Krames, *Appl. Phys. Lett.* **89**, 071109 (2006).

<sup>5</sup>H. Kim, J. Cho, J. W. Lee, S. Yoon, H. Kim, C. Sone, and Y. Park, *Appl. Phys. Lett.* **90**, 161110 (2007).

<sup>6</sup>C. H. Kuo, H. C. Feng, C. W. Kuo, C. M. Chen, L. W. Wu, and G. C. Chi, *Appl. Phys. Lett.* **90**, 142115 (2007).

<sup>7</sup>J. J. Wierer, M. R. Krames, J. E. Epler, N. F. Gardner, M. G. Craford, J. R. Wendt, J. A. Simmons, and M. M. Sigalas, *Appl. Phys. Lett.* **84**, 3885 (2004).

<sup>8</sup>M.-K. Kwon, J.-Y. Kim, I.-K. Park, K. S. Kim, G.-Y. Jung, S.-J. Park, J. W. Kim, and Y. C. Kim, *Appl. Phys. Lett.* **92**, 251110 (2008).

<sup>9</sup>J. K. Kim, S. Chhajed, M. F. Schubert, E. F. Schubert, A. J. Fischer, M. H. Crawford, J. Cho, H. Kim, and C. Sone, *Adv. Mater. (Weinheim, Ger.)* **20**, 801 (2008).

<sup>10</sup>T. S. Oh, Seung H. Kim, T. K. Kim, Y. S. Lee, H. Jeong, G. M. Yang, and E.-K. Suh, *Jpn. J. Appl. Phys., Part 1* **47**, 5333 (2008).

<sup>11</sup>C.-F. Lin, Z.-J. Yang, B.-H. Chin, J.-H. Zheng, J.-J. Dai, B.-C. Shieh, and C.-C. Chang, *J. Electrochem. Soc.* **153**, G1020 (2006).

<sup>12</sup>H. W. Jang, J. H. Son, and J.-L. Lee, *Appl. Phys. Lett.* **90**, 012106 (2007).

<sup>13</sup>J. H. Son, G. H. Jung, and J.-L. Lee, *Appl. Phys. Lett.* **93**, 012102 (2008).

<sup>14</sup>D. J. Poxson, F. W. Mont, M. F. Schubert, J. K. Kim, and E. F. Schubert, *Appl. Phys. Lett.* **93**, 101914 (2008).